Supplementary Data

Unravelling dispersion forces in liquid-phase enantioseparation. Part I: Impact of ferrocenyl versus phenyl groups

Barbara Sechi,[a,#] Alessandro Dessì,[a,#] Roberto Dallocchio,[a,#] Nutsa Tsetskhladze,[b] Bezhan

Chankvetadze,[b] Mireia Pérez-Baeza,[c] Sergio Cossu,[d] Giorgi Jibuti,[b] Victor Mamane,[e,*] and Paola

Peluso[a,*]

[a] Istituto di Chimica Biomolecolare ICB-CNR, Sede secondaria di Sassari, Traversa La Crucca 3, Regione Baldinca,
Li Punti, 07100 Sassari, Italy
[b] Institute of Physical and Analytical Chemistry, School of Exact and Natural Sciences, Tbilisi State University,
Chavchavadze Ave 3, 0179 Tbilisi, Georgia
[c] Departamento de Química Analítica, Universitat de València, Burjassot, València, Spain
[d] Dipartimento di Scienze Molecolari e Nanosistemi DSMN, Università Ca' Foscari Venezia, Via Torino 155, I-30172
Mestre Venezia, Italy
[e] Institut de Chimie de Strasbourg, UMR CNRS 7177, Equipe LASYROC, 1 rue Blaise Pascal, 67008 Strasbourg Cedex,
France
* Corresponding authors. E-mail address: paola.peluso@cnr.it (P. Peluso); vmamane@unistra.fr (V. Mamane).
[#] These authors contributed equally to this work.

<div align="center">

Table of contents

</div>

S1. Additional introductive details

Table S1. Chiral columns and selectors used for the enantioseparations of analytes **1** and **2**. Calculated $V_{S,max}$ and $V_{S,min}$ (au) values on a 0.002 au electron density isosurface for the main recognition sites (N-H as hydrogen bond (HB) donor, and C=O as HB acceptor) are reported (DFT/B3LYP/6-311G*).
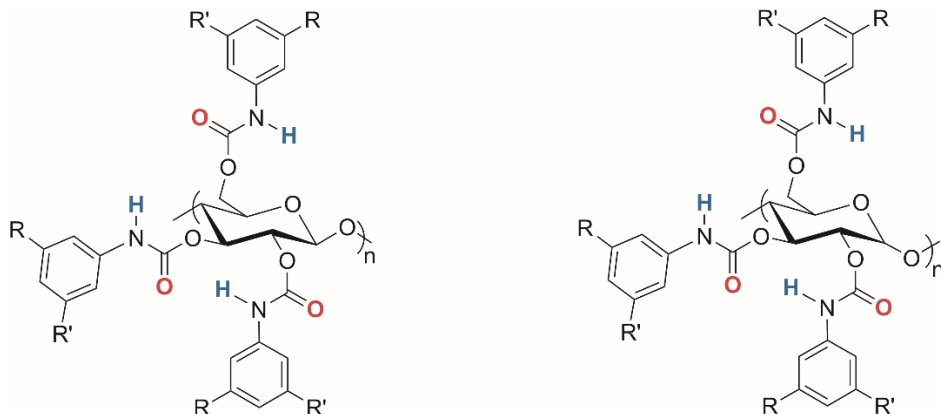
cellulose carbamate-based selectors   amylose carbamate-based selectors

Column[a]		Chiral selector	V (au)	
Name	Type	Name	$V_{S,max}$ N-<u>H</u>	$V_{S,min}$ C=<u>O</u>
Lux Cellulose-1	coated	cellulose *tris*(3,5-dimethylphenylcarbamate)	0.0788	-0.0660
Lux i-Cellulose-5	immobilized	cellulose *tris*(3,5-dichlorophenylcarbamate)	0.0950	-0.0561
Lux Amylose-1	coated	amylose *tris*(3,5-dimethylphenylcarbamate)	0.0788	-0.0660
Lux i-Amylose-1	immobilized	amylose *tris*(3,5-dimethylphenylcarbamate)	0.0788	-0.0660
Lux i-Amylose-3	immobilized	amylose *tris*(3-chloro-5-methylphenylcarbamate)	0.0871	-0.0594

[a] Lux series columns (Phenomenex)

S2. Additional computational details

Models of amylose carbamate-based selectors - The Gaussian 09 program (DFT, B3LYP, 3–21G*) [1] was used for the *ab initio* geometry optimization calculation of the monomeric units of α-D-glucose-1,4-dimethoxy-*tris*(3,5-dimethylphenylcarbamate), - *tris*(4-methylphenylcarbamate), and *tris*(2,5-dimethylphenylcarbamate). The optimized structures were used to build nonamers (9-mer) of the corresponding amylose-based polymers [2]. The amylose-based polymers were characterized by a 4/3 left-handed helical structure according to the structure reported by Okamoto and co-authors [3, 4], setting the dihedral angles of the units, defined by H_1–C_1–O–$C_{4'}$ and $H_{4'}$–$C_{4'}$–O–C_1 to −68.5° and −42.0°. The terminal residues of the polymers were closed with methoxyl groups. The polymer structures were energy-minimized using the GAFF force-fields with AM1-BCC charges assigned with the AMBER18 Antechamber toolkit (University of California, San Francisco, USA) [5].

Model of ferrocene and benzene - The Gaussian 09 program (DFT, B3LYP, 6–311G*) [1] was used for the *ab initio* geometry optimization calculation of the monomeric units of ferrocene and benzene. The nonamer (9-mer) of the α-D-glucose-1,4-dimethoxy-*tris*(3,5-dimethylphenylcarbamate) was prepared as reported in the previous paragraph. Ferrocene and benzene were energy-minimized using the GAFF force-fields with RESP charges assigned with Gaussian 09.

MD simulations of ferrocene- and benzene-amylose nonamer complexes - The prepared structures were used in the final MD simulations. The initial position of the aromatic guests was determined by molecular docking. Solvent effect was considered by means of the explicit periodic solvent box (*n*-hexane/2-PrOH 90:10). In this regard, polysaccharide-analyte complexes were prepared for MD runs by solvating the system with an octahedral box with a 20 Å radius polysaccharide cutoff by using Packmol-70 memgen [6,7] and an in-house script to manage solvent mixtures. Finally, the production step was carried out under the equilibrium conditions, and the system was subjected to 100 ns MD simulation for the aromatic guests on the polymer nonamer. 100 ns of the trajectories from each case were considered for statistical analysis.

[1]   M.J. Frisch, G.W. Trucks, H.B. Schlegel, G.E. Scuseria, M.A. Robb, J.R. Cheeseman, G. Scalmani, V. Barone, B. Mennucci, G.A. Petersson, H. Nakatsuji, M. Caricato, X. Hratchian, H.P. Li, A.F. Izmaylov, J. Bloino, G. Zheng, J.L. Sonnenberg, M. Hada, M. Ehara, K. Toyota, R. Fukuda, J. Hasegawa, M. Ishida, T. Nakajima, Y. Honda, O. Kitao, H. Nakai, T. Vreven, J.A. Montgomery Jr, J.E. Peralta, F. Ogliaro, M. Bearpark, J.J. Heyd, E. Brothers, K.N. Kudin, V.N. Staroverov, T. Keith, R. Kobayashi, J. Normand, K. Raghavachari, A. Rendell, J.C. Burant, S.S. Iyengar, J. Tomasi, M. Cossi, N. Rega, J.M. Millam, M. Klene, J.E. Knox, J.B. Cross, V. Bakken, C. Adamo, J. Jaramillo, R. Gomperts, R.E. Stratmann, O. Yazyev, A.J. Austin, R. Cammi, C. Pomelli, J.W. Ochterski, R.L. Martin, K. Morokuma, V.G. Zakrzewski, G. Voth, P. Salvador, J.J. Dannenberg, S. Dapprich, A.D. Daniels, O. Farkas, J.B. Foresman, J. Ortiz, J. Cioslowski, D.J. Fox, Gaussian 09, Revision B. 01, Inc.Gaussian, C.T. Wallingford, 2010.
[2]   P. Peluso, V. Mamane, R. Dallocchio, A. Dessì, R. Villano, D. Sanna, E. Aubert, P. Pale, S. Cossu, Polysaccharide-based chiral stationary phases as halogen bond acceptors: A novel strategy for detection of stereoselective σ-hole bonds in solution, J. Sep. Sci. 41 (2018) 1247–1256.
[3]   C. Yamamoto, E. Yashima, Y. Okamoto, Structural analysis of amylose tris(3,5-dimethylphenylcarbamate) by NMR relevant to its chiral recognition mechanism in HPLC, J. Am. Chem. Soc. 124 (2002) 12583–12589.
[4]   Y.K. Ye, S. Bai, S. Vyas, M.J. Wirth, NMR and computational studies of chiral discrimination by amylose *tris*(3,5-dimethylphenylcarbamate), J. Phys. Chem. B 111 (2007) 1189–1198.
[5]   D.A. Case, I.Y. Ben-Shalom, S.R. Brozell, D.S. Cerutti, T.E. Cheatham III, V.W.D. Cruzeiro, T.A. Darden, R.E. Duke, D. Ghoreishi, M.K. Gilson, H. Gohlke, A.W. Goetz, D. Greene, R. Harris, N. Homeyer, Y. Huang, S. Izadi, A. Kovalenko, T. Kurtzman, T.S. Lee, S. LeGrand, P. Li, C. Lin, J. Liu, T. Luchko, R. Luo, D.J. Mermelstein, K.M. Merz, Y. Miao, G. Monard, C. Nguyen, H. Nguyen, I. Omelyan, A. Onufriev, F. Pan, R. Qi, D.R. Roe, A. Roitberg, C. Sagui, S. Schott-Verdugo, J. Shen, C.L. Simmerling, J. Smith, R. Salomon-Ferrer, J. Swails, R.C. Walker, J. Wang, H. Wei, R.M. Wolf, X. Wu, L. Xiao, D.M. York, P.A. Kollman, AMBER 2018, University of California, San Francisco, 2018.
[6]   J.M. Martínez, L. Martínez, Packing optimization for automated generation of complex system's initial configurations for molecular dynamics and docking, J. Comput. Chem. 24 (2003) 819–825.
[7]   L. Martínez, R. Andrade, E.G. Birgin, J.M. Martínez, PACKMOL: A package for building initial configurations for molecular dynamics simulations, J. Comput. Chem. 30 (2009) 2157–2164.

S3. Additional HPLC data

Table S2. Retention times (t, min), retention factors (k), selectivity factors (α) and enantiomer elution order (EEO) of compounds **1** and **2** on Lux Cellulose-1, i-Cellulose-5, Amylose-1, i-Amylose-1, and i-Amylose-3 with n-hexane/2-PrOH 90:10 v/v as mobile phase (flow rate = 0.8 ml/min, T = 25 °C).

analyte	chiral column	t_1	t_2	k_1	k_2	α	EEO
1	Cellulose-1	10.559	10.559	1.96	1.96	1.00	--
	i-Cellulose-5	17.636	51.770	3.85	13.23	3.44	*M-P*
	Amylose-1	24.679	111.362	6.23	31.60	5.08	*M-P*
	i-Amylose-1	16.667	30.064	3.69	7.462	2.02	*M-P*
	i-Amylose-3	30.510	57.663	7.50	15.06	2.01	*M-P*
2	Cellulose-1	6.346	11.727	0.78	2.29	2.94	*M-P*
	i-Cellulose-5	8.308	8.308	1.28	1.28	1.00	--
	Amylose-1	10.495	10.753	2.07	2.15	1.04	*M-P*
	i-Amylose-1	8.917	9.286	1.51	1.61	1.07	*M-P*
	i-Amylose-3	9.873	10.468	1.75	1.92	1.10	*M-P*
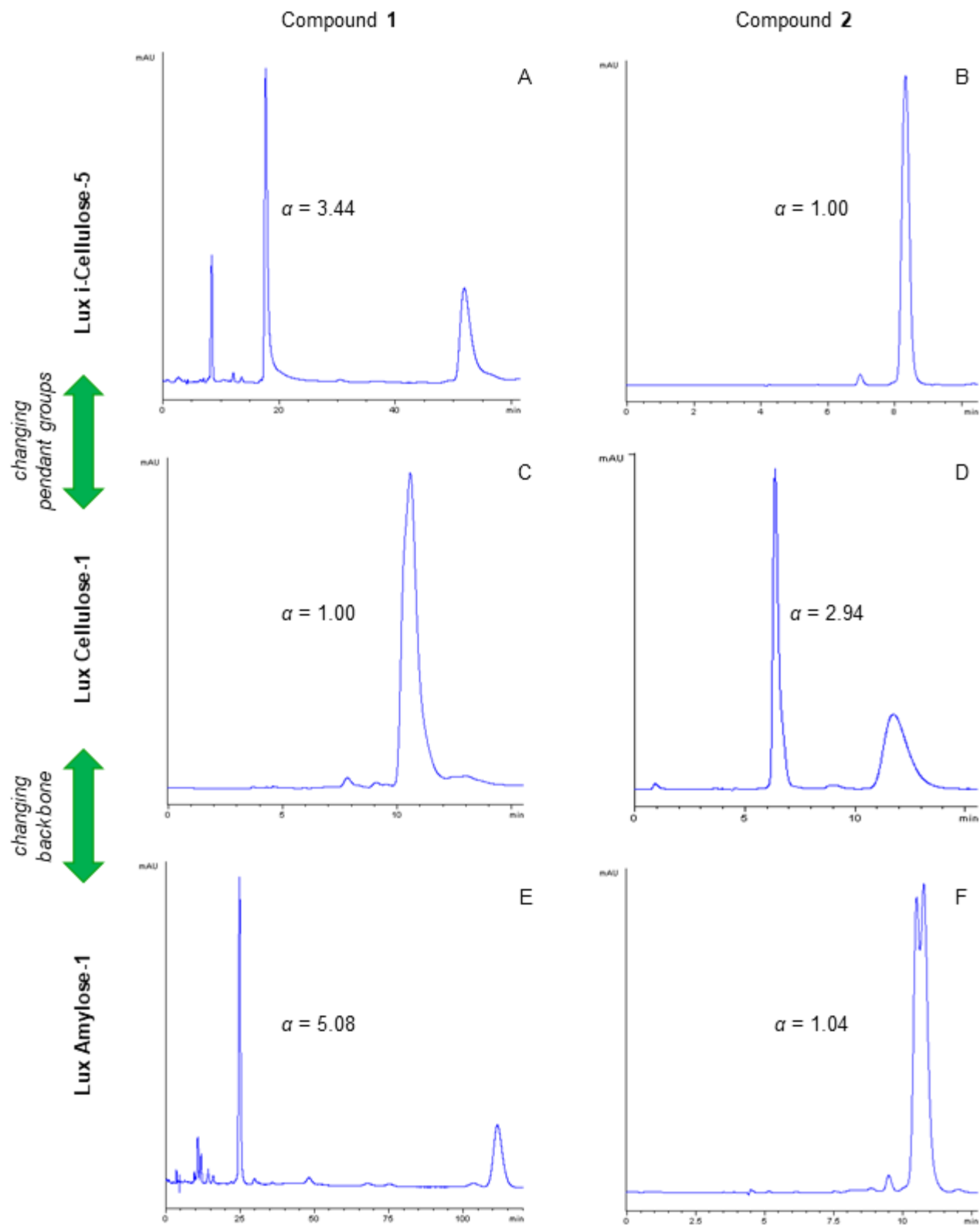
Fig. S1. Chromatographic traces of the enantioseparation of compounds **1** and **2** (EEO, *M-P*) on Lux i-Cellulose-5 (A,B), Lux Cellulose-1 (C,D), and Lux Amylose-1 (E,F) (*n*-hexane/2-PrOH 90:10 v/v, flow rate = 0.8 ml/min, T = 25 °C).

Table S3. Retention times (*t*, min), retention factors (*k*), selectivity factors (α) and enantiomer elution order (EEO) of compounds **1** and **2** on Lux Cellulose-1 with *n*-hexane/2-PrOH 90:10 v/v (A) and *n*-hexane/2-PrOH/MeOH 90:5:5 v/v/v (B) as mobile phases, and i-Amylose-1 with A, B, and pure MeOH (C) as mobile phases (flow rate = 0.8 ml/min, T = 25 °C).

analyte	chiral column	MP	t_1	t_2	k_1	k_2	α	EEO
1	Cellulose-1	A	10.559	10.559	1.96	1.96	1.00	--
		B	9.463	9.961	1.68	1.82	1.08	*M-P*
	i-Amylose-1	A	16.667	30.064	3.69	7.46	2.02	*M-P*
		B	12.935	15.115	2.55	3.15	1.24	*M-P*
		C	13.134	14.769	2.38	2.80	1.18	*M-P*
2	Cellulose-1	A	6.346	11.727	0.78	2.29	2.94	*M-P*
		B	6.830	10.726	0.93	2.04	2.18	*M-P*
	i-Amylose-1	A	8.917	9.286	1.51	1.61	1.07	*M-P*
		B	7.268	7.484	0.99	1.05	1.06	*M-P*
		C	6.898	6.898	0.77	0.77	1.00	--

Thermodynamics

The dependence between retention/selectivity and the temperature of the chiral separation is described by the following equations (1,2):

$$\ln k = -\Delta H^\circ/RT + \Delta S^\circ/R + \ln \Phi \tag{1}$$

$$\ln \alpha = -\Delta\Delta H^\circ/RT + \Delta\Delta S^\circ/R \tag{2}$$

where k is the retention factor, R is the gas constant, T is the absolute temperature, Φ is the phase ratio, and α is selectivity. ΔH° and ΔS° represent the differences in the enthalpy and entropy, respectively, when one enantiomer transfers from mobile phase to the stationary phase. Here, ΔS^* is used to substitute the expression $\Delta S^\circ/R + \ln \Phi$. Assuming that the plots of $\ln k$ against $1/T$ is linear in the temperature range of this study, the correlative thermodynamic parameters, which are temperature-independent, could be derived from the slope ($\Delta H^\circ = -$ slope $\times R$) and the intercept ($\Delta S^* =$ intercept $\times R$) of the straight lines. $\Delta\Delta H^\circ$ and $\Delta\Delta S^\circ$ represent the enthalpic and the entropic terms, respectively, contributing to the difference between the free energies of transfer of the two enantiomers from the mobile phase to the CSP, according to the Gibbs-Helmholtz equation (3):

$$\Delta\Delta G^\circ = \Delta\Delta H^\circ - T\Delta\Delta S^\circ \tag{3}$$

The knowledge of $\Delta\Delta H^\circ$ and $\Delta\Delta S^\circ$ allows for calculating the isoenantioselective temperature (T_{iso}):

$$T_{iso} = \Delta\Delta H^\circ/\Delta\Delta S^\circ \tag{4}$$

At this temperature, the enthalpic and the entropic terms of equation (3) compensate each other, the free energy term is zero and the enantiomers co-elute. In general, enantioseparations at lower temperatures than T_{iso} are enthalpy-driven, whereas they are entropy-driven at higher temperatures. By changing the temperature between the two regions, an EEO reversal occurs.

The enthalpy/entropy ratio (5)

$$Q = \Delta\Delta H^\circ/(298.15 \times \Delta\Delta S^\circ) \tag{5}$$

describes the relative contribution to the free energy of adsorption.

Table S4. Temperature dependence of retention factors and van't Hoff equations for analytes **1** and **2** on Lux Cellulose-1, i-Cellulose-5, Amylose-1, i-Amylose-1, i-Amylose-3 (flow rate = 0.8 ml/min), temperature range 278.15-318.15 K. Mobile phase: *n*-hexane/2-PrOH 90:10 v/v.

| bipy | k | \multicolumn{9}{c}{Temperature (K)} | Regression equation | $r^{2\,a}$ |
		278.15	283.15	288.15	293.15	298.15	303.15	308.15	313.15	318.15		
Lux Cellulose-1		
1	k_M	2.84	2.56	2.30	2.07	1.96	1.80	1.66	1.55	1.46	ln k_M = 1467.56x − 4.2505	0.9962
	k_P	3.07	2.71	2.41	2.17	1.96	1.80	1.66	1.55	1.46	ln k_P = 1653.58x − 4.8501	0.9943
	α	1.08	1.06	1.05	1.05	1.00	1.00	1.00	1.00	1.00	ln α = 238.39x − 0.7786	0.9106
2	k_M	0.98	0.92	0.87	0.82	0.78	0.74	0.71	0.68	0.65	ln k_M = 919.84x − 3.3301	0.9985
	k_P	3.03	2.88	2.71	2.50	2.29	2.07	2.01	1.81	1.61	ln k_P = 1385.59x − 3.8339	0.9837
	α	3.08	3.12	3.12	3.06	2.94	2.80	2.84	2.68	2.48	ln α = 465.59x − 0.5017	0.8338
Lux i-Cellulose-5		
1	k_M	7.00	5.86	5.03	4.38	3.85	3.39	3.05	2.76	2.53	ln k_M = 2246.51x − 6.1674	0.9958
	k_P	52.37	35.89	24.94	18.04	13.23	9.57	7.28	5.62	4.48	ln k_P = 5470.24x − 15.748	0.9987
	α	7.49	7.10	4.96	4.12	3.44	2.82	2.39	2.04	1.77	ln α = 3223.15x − 9.5785	0.9996
2	k	2.09	1.82	1.59	1.42	1.28	1.17	1.07	0.99	0.91	ln k = 662.92x − 2.3153	0.9912
Lux Amylose-1		
1	k_M	7.47	7.04	6.72	6.42	6.22	5.92	5.75	5.52	5.40	ln k_M = 716.50x − 0.5769	0.9956
	k_P	52.54	45.63	40.33	35.34	31.60	27.28	24.39	21.43	19.37	ln k_P = 2220.98x − 4.0158	0.9992
	α	7.03	6.48	6.00	5.50	5.08	4.61	4.24	3.88	3.59	ln α = 1502.98x − 3.4340	0.9971
2	k_M	2.79	2.57	2.39	2.19	2.07	1.93	1.85	1.75	1.69	ln k_M = 1120.76x − 3.0204	0.9934
	k_P	2.79	2.57	2.39	2.25	2.15	2.02	1.94	1.85	1.80	ln k_P = 962.27x − 2.4574	0.9917
	α	1.00	1.00	1.00	1.03	1.04	1.05	1.05	1.06	1.06	ln α = -155.47x + 0.5539	0.9117
Lux i-Amylose-1		
1	k_M	5.08	4.66	4.30	3.97	3.69	3.41	3.19	3.01	2.76	ln k_M = 1329.87x − 3.1559	0.9994
	k_P	11.79	10.47	9.34	8.30	7.46	6.64	5.98	5.47	4.70	ln k_P = 1990.04x − 4.6755	0.9977
	α	2.32	2.25	2.17	2.09	2.02	1.94	1.87	1.82	1.70	ln α = 663.04x − 1.5296	0.9882
2	k_M	2.07	1.89	1.76	1.61	1.51	1.38	1.30	1.23	1.15	ln k_M = 1303.49x − 3.9633	0.9990
	k_P	2.15	1.99	1.86	1.72	1.61	1.48	1.40	1.32	1.24	ln k_P = 1221.34x − 3.6239	0.9991
	α	1.04	1.05	1.06	1.06	1.07	1.07	1.08	1.08	1.08	ln α = -83.99x + 0.3457	0.9380
Lux i-Amylose-3		
1	k_M	10.43	9.58	8.84	8.04	7.50	6.76	6.37	5.94	5.61	ln k_M = 1402.02x − 2.6943	0.9982
	k_P	25.25	22.16	19.52	16.89	15.06	12.94	11.72	10.53	9.61	ln k_P = 2182.00x − 4.6127	0.9987
	α	2.42	2.31	2.21	2.10	2.01	1.91	1.84	1.77	1.71	ln α = 782.76x − 1.9283	0.9991
2	k_M	2.49	2.26	2.06	1.88	1.75	1.58	1.51	1.42	1.36	ln k_M = 1370.49x − 4.0312	0.9938
	k_P	2.74	2.48	2.26	2.06	1.92	1.73	1.65	1.54	1.47	ln k_P = 1401.45x − 4.0457	0.9949
	α	1.10	1.10	1.10	1.10	1.09	1.09	1.09	1.09	1.08	ln α = 37.53x − 0.0369	0.8027

[a]r^2, correlation coefficient of van't Hoff plot ln k (1/T) and ln α (1/T).

Table S5. Thermodynamic parameters calculated from the van't Hoff plots (temperature range 278.15-318.15 K) for analytes **1** and **2** on Lux Cellulose-1, i-Cellulose-5, Amylose-1, i-Amylose-1, and i-Amylose-3 (flow rate = 0.8 ml/min), temperature range 278.15-318.15 K. Mobile phase: *n*-hexane/2-PrOH 90:10 v/v.

Bipy		ln k vs 1/T		ln α vs 1/T		
		ΔH (cal·mol^{-1})	ΔS^* (cal·K^{-1}·mol^{-1})	$\Delta\Delta H$ (cal·mol^{-1})	$\Delta\Delta S$ (cal·K^{-1}·mol^{-1})	T_{iso}, K (Q^a)
			Lux Cellulose-1			
1	*M*	-2916.0 ± 67.8	-8.44 ± 0.22	-473.7 ± 85.7	-1.55 ± 0.30	305.6 (1.02)
	P	-3285.7 ± 94.3	-9.64 ± 0.32			
2	*M*	-1827.72 ± 26.4	-6.62 ± 0.09	-925.1 ±156.1	-1.00 ± 0.52	925.1 (3.10)
	P	-2753.17 ± 134.1	-7.62 ± 0.45			
			Lux i-Cellulose-5			
1	*M*	-4463.82 ± 109.4	-12.25 ± 0.37	-6404.4 ±49.4	-19.03 ± 0.17	336.5 (1.13)
	P	-10869.37 ± 147.3	-31.29 ± 0.50			
2	-	-1317.22 ± 46.8	-4.60 ± 0.16	--	--	--
			Lux Amylose-1			
1	*M*	-1423.69 ± 35.6	-1.15 ± 0.12	-2986.4 ± 60.5	-6.82 ± 0.20	437.9 (1.47)
	P	-4413.09 ± 46.3	-7.98 ± 0.16			
2	*M*	-2226.95 ± 68.7	-6.00 ± 0.23	308.92 ± 36.3	1.10 ± 0.12	280.8 (0.94)
	P	-1912.03 ± 66.1	-4.88 ± 0.22			
			Lux i-Amylose-1			
1	*M*	-2642.45 ± 24.7	-6.27 ± 0.83	-1317.46 ± 54.5	-3.04 ± 0.18	433.4 (1.45)
	P	-3954.21 ± 72.1	-9.29 ± 0.24			
2	*M*	-2590.03 ± 30.3	-7.88 ± 0.10	166.90 ± 16.2	0.69 ± 0.05	241.9 (0.81)
	P	-2426.80 ± 27.0	-7.20 ± 0.09			
			Lux i-Amylose-3			
1	*M*	-2785.81 ± 44.9	-5.35 ± 0.15	-1555.35 ± 17.3	-3.83 ± 0.06	406.1 (1.36)
	P	-4335.63 ± 59.2	-9.17 ± 0.20			
2	*M*	-2723.16 ± 81.1	-8.01 ± 0.27	-74.58 ± 13.97	-0.07 ± 0.05	1065.4 (3.57)
	P	-2784.68 ± 75.2	-8.04 ± 025			

^{a} $Q = \Delta\Delta H°/(298.15 \times \Delta\Delta S°)$, thermodynamic ratio
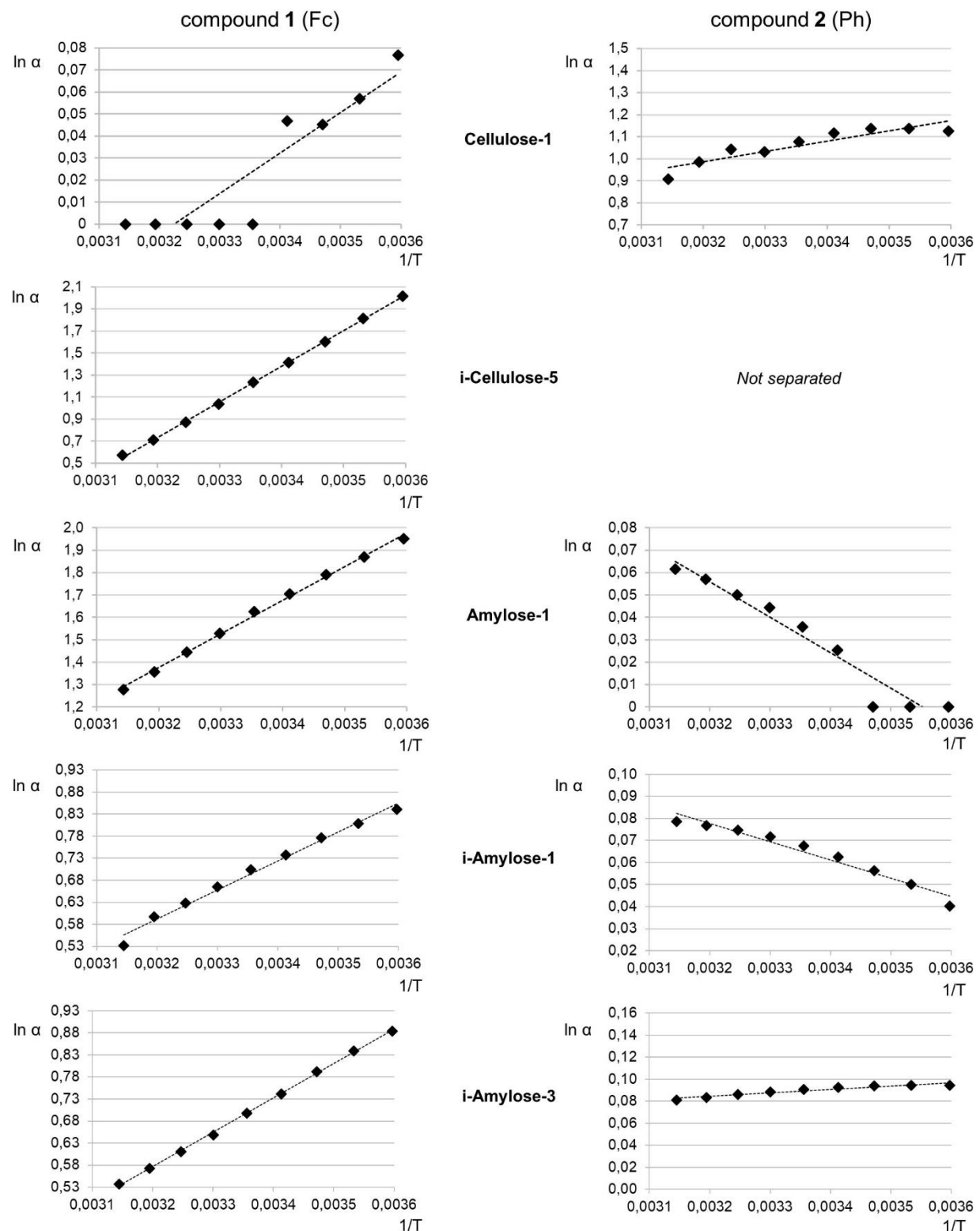
Fig. S2. ln α vs. 1/T van't Hoff plots for the enantioseparation of **1** and **2** on Lux Cellulose-1, i-Cellulose-5, Amylose-1, i-Amylose-1, and i-Amylose-3 (*n*-hexane/2-PrOH 90:10 v/v, 0.8 ml/min, temperature range 278.15-318.15 K) (for chromatographic parameters see Table S5).
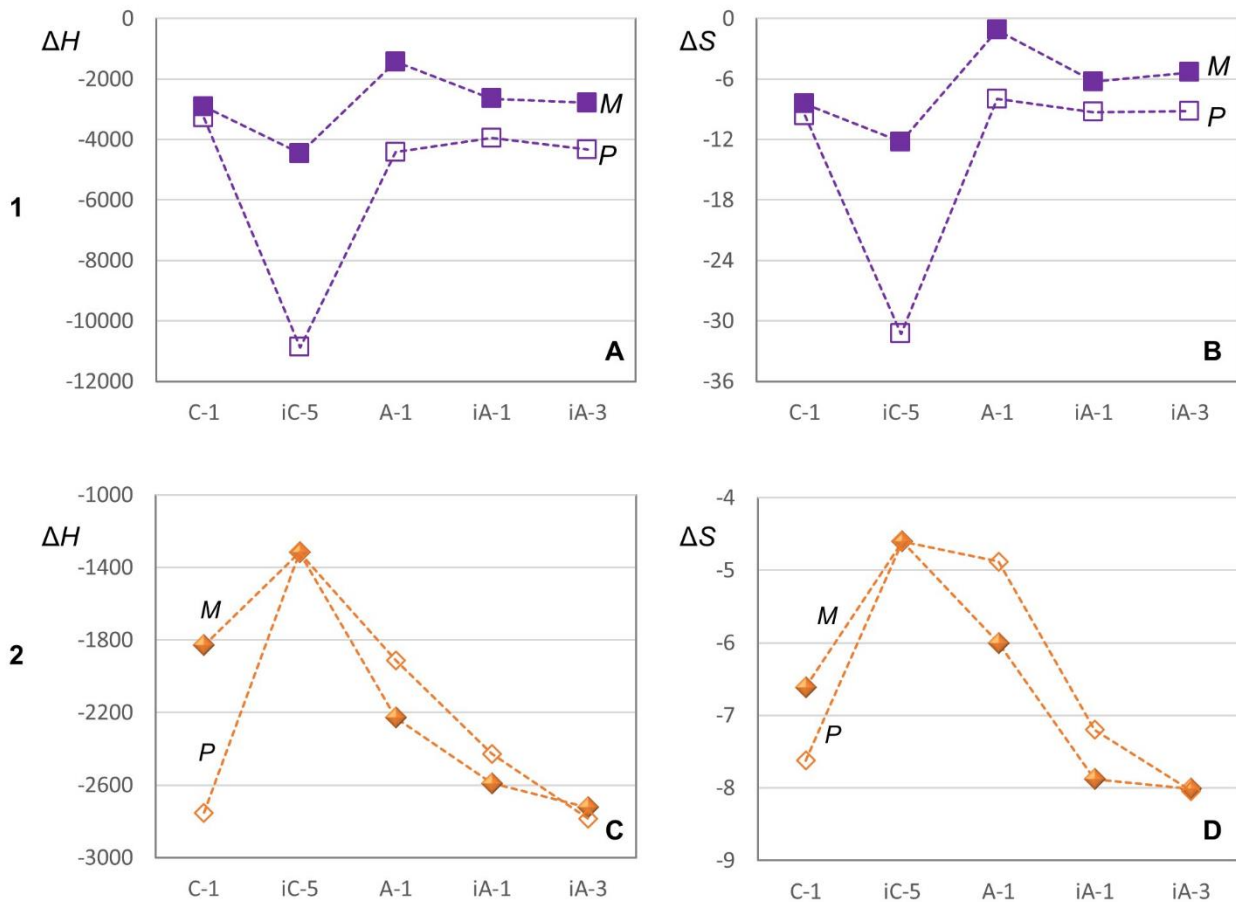
Fig. S3. Changes of ΔH and ΔS for adsorption of (*M*)- and (*P*)-enantiomers of compounds **1** (A,B) and **2** (C,D) on Lux Cellulose-1, i-Cellulose-5, Amylose-1, i-Amylose-1, and i-Amylose-3 (*n*-hexane/2-PrOH 90:10 v/v, 0.8 ml/min, temperature range 278.15-318.15 K) (for thermodynamics parameters see Table S5).